

Effect of Topologically Controlled Coulombic Interactions on the Dynamic Behavior of Photoexcited Nitrophenyl Alkyl Ethers in the Presence of Tertiary Amines with Limited Motion Freedom

Roberto Gonzalez-Blanco, José L. Bourdelande,* and Jordi Marquet*

Department of Chemistry, Universitat Autònoma de Barcelona, 08193 Bellaterra, Barcelona, Spain

Received September 24, 1996[®]

Time-resolved electronic absorption spectroscopy has been successfully applied to clarify the mechanism of the “abnormal” photochemical cleavage of 4-nitrophenyl piperidinoalkyl ethers induced by controlled Coulombic disturbance of the “normal” electronic distribution of the radical anion intermediate. Thus, photolysis of 1-piperidino-2-(2-methoxy-4-nitrophenoxy)ethane (a system with an amine with limited freedom of motion) in acetonitrile leads to C–O bond photocleavage in a relatively slow process ($k \approx 4 \times 10^5 \text{ s}^{-1}$) from intermediate species that show radical-ion pair behavior. Systems with higher freedom of motion of the amine moiety, such as 1-piperidino-5-(2-methoxy-4-nitrophenoxy)pentane or 4-nitroveratrole + triethylamine, show the intermediate radical-ion pairs mainly evolving to reduction products, probably a result of intermediates with geometries not allowed for the system with limited freedom of motion of the amine.

The electron distribution in reactive intermediates largely determines the outcome of a chemical or photochemical reaction. However, the effect of the counterion on the outcome of a chemical process (“metal ion catalysis”, “electrophilic catalysis”, etc.) has been traditionally attributed¹ to Lewis acid complexation, ignoring the important associated electrostatic effect. Only recently has this electrostatic effect been recognized as responsible for the lowest energy conformation of the radical anion/cation pair in alkyl aryl ethers² and the acceleration of the electrocyclic reactions by metal cation complexation.³

In 1991, we predicted that the Coulombic alteration of the “normal” electron distribution of a charged intermediate could lead to previously unknown processes.^{4a} The idea was applied to achieve the previously unknown reductive cleavage of certain ethers.⁴

The reductive cleavage of alkyl aryl ethers⁵ is an important process in chemistry that has lately received attention from both the synthetic⁶ and mechanistic⁷ points of view. The first reaction step leads to radical anions, ROAr^{•-}, known since 1968 from ESR studies.⁸ Dianions were also discussed in the past as intermedi-

ates⁹ although more recent literature^{5,7} showed that, in most cases, this is an unnecessary hypothesis.

Intermediates of the ROAr^{•-} type share many common features with the aryl and benzyl halide radical anions important in S_{RN}1 reactions.¹⁰ Symons,¹¹ Bunnett,¹² Rossi,¹³ Savéant,¹⁴ and others¹⁵ have proposed that cleavage of C–X bonds in halogeno-aromatic radical anions may be seen as the result of electron transfer from the π^* radical anion to the σ^* aryl nucleofugal bond by an orbital crossing. Efficient fragmentation in aryl and benzyl halides depends on a delicate balance. Thus, electron-attracting groups that stabilize the π^* orbitals making easier the initial electron transfer can also prevent the $\pi^*-\sigma^*$ crossing by increasing the energy gap. When a cyano group replaces the nitro group either in *p*-nitroaryl or *p*-nitrobenzyl halides, the rate of dissociation of the radical-anion, as measured by pulse radiolysis,¹⁶ increases by at least five orders of magnitude.

For alkyl aryl ether radical anions, the efficiency and selectivity of the fragmentation depends on the probability of transition from the π^* state to the σ^* state. In addition a new feature, called the “spin regioconservation principle”, must be taken into account.¹⁷ Guthrie and Maslak proposed such a concept based on fragmentation studies of aryl nitrobenzyl and benzyl nitroaryl ethers. These authors state that the fission of alkyl aryl ether

[®] Abstract published in *Advance ACS Abstracts*, August 15, 1997.

(1) (a) Pregel, M. J.; Buncel, E. *J. Org. Chem.* **1991**, *56*, 5583. (b) Dunn, E. J.; Moir, R. Y.; Buncel, E.; Purdon, J. G.; Bannard, R. A. *Can. J. Chem.* **1990**, *68*, 1837. (c) Breslow, R.; Guo, T. *J. Am. Chem. Soc.* **1988**, *110*, 5613. (d) Casaschi, A.; Desimoni, G.; Faita, G.; Invernizzi, A. G.; Lanati, S.; Righetti, P. P. *J. Am. Chem. Soc.* **1993**, *115*, 8002.

(2) Lazana, M. C. R. L. R.; Franco, M. L. T. M. B.; Herold, B. J. *J. Am. Chem. Soc.* **1989**, *111*, 8640.

(3) (a) Jiao, H.; Schleyer, P. v.R. *Angew. Chem., Int. Ed. Engl.* **1993**, *32*, 1760. (b) Jiao, H.; Schleyer, P. v.R. *J. Chem. Soc., Faraday Trans.* **1994**, *90*, 1559. (c) Jiao, H.; Schleyer, P. v.R. *J. Am. Chem. Soc.* **1995**, *117*, 11529.

(4) (a) Cayón, E.; Marquet, J.; Lluch, J. M.; Martín, X. *J. Am. Chem. Soc.* **1991**, *113*, 8970. (b) Marquet, J.; Cayón, E.; Martín, X.; Casado, F.; Gallardo, I.; Moreno, M.; Lluch, J. M. *J. Org. Chem.* **1995**, *60*, 3814.

(5) (a) Burwell Jr., R. L. *Chem. Rev.* **1954**, *54*, 615. (b) Bhatt, M. V.; Kulkarni, S. U. *Synthesis* **1983**, 249. (c) Maercker, A. *Angew. Chem., Int. Ed. Engl.* **1987**, *26*, 972.

(6) (a) Azzena, U.; Melloni, G.; Pisano, L. *Tetrahedron Lett.* **1993**, *34*, 5635. (b) Azzena, U.; Melloni, G.; Pisano, L.; Sechi, B. *Tetrahedron Lett.* **1994**, *35*, 6759. (c) Azzena, U.; Demartis, S.; Fiori, M. G.; Melloni, G.; Pisano, L. *Tetrahedron Lett.* **1995**, *36*, 8123.

(7) (a) Koppang, M. D.; Woolsley, N. F.; Bartak, D. E. *J. Am. Chem. Soc.* **1984**, *106*, 2799. (b) Thorton, T. A.; Woolsley, N. F.; Bartak, D. E. *J. Am. Chem. Soc.* **1986**, *108*, 6497. (c) Azzena, U.; Denurra, T.; Melloni, G.; Fenude, E.; Rassu, G. *J. Org. Chem.* **1992**, *57*, 1444.

(8) Bowers, K. W. In *Radical Ions*; Kaiser, E. T., Kevan, L., Eds.; Wiley: New York, 1968; p 232.

(9) (a) Birch, A. J. *J. Chem. Soc.* **1944**, 430. (b) Birch, A. J. *J. Chem. Soc.* **1947**, 102. (c) Eisch, J. J. *J. Org. Chem.* **1963**, *28*, 707. (d) Itoh, M.; Yoshida, S.; Ando, T.; Miyaura, N. *Chem. Lett.* **1976**, 271. (e) Testaferri, L.; Tiecco, M.; Tingoli, M.; Chianelli, D.; Montanucci M. *Tetrahedron* **1982**, *38*, 3687.

(10) (a) Kornblum, N. *Angew. Chem., Int. Ed. Engl.* **1975**, *14*, 734. (b) Bunnett, J. F. *Acc. Chem. Res.* **1978**, *11*, 413. (c) Savéant, J. M. *Adv. Phys. Org. Chem.* **1990**, *26*, 1.

(11) Symons, M. C. R. *Pure Appl. Chem.* **1981**, *53*, 223. (12) Bunnett, J. F.; Creary, X. *J. Org. Chem.* **1975**, *40*, 3740.

(13) (a) Villar, H.; Castro, E. A.; Rossi, R. A. *Can. J. Chem.* **1982**, *60*, 2525. (b) Villar, H.; Castro, E. A.; Rossi, R. A. *Z. Naturforsch.* **1984**, *39a*, 49.

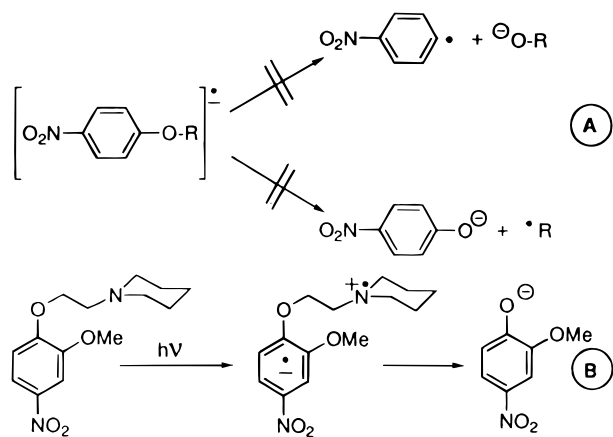
(14) Andrieux, C. P.; Savéant, J. M.; Tallec, A.; Tardivel, R.; Tardy, C. *J. Am. Chem. Soc.* **1996**, *118*, 9788.

(15) Pierini, A. B.; Duca, J. S., Jr. *J. Chem. Soc., Perkin Trans. 2* **1995**, 1821.

(16) Neta, P.; Behar, D. *J. Am. Chem. Soc.* **1981**, *103*, 103.

(17) (a) Maslak, P.; Guthrie, R. D. *J. Am. Chem. Soc.* **1986**, *108*, 2628. (b) *Idem.* *J. Am. Chem. Soc.* **1986**, *108*, 2637.

Scheme 1



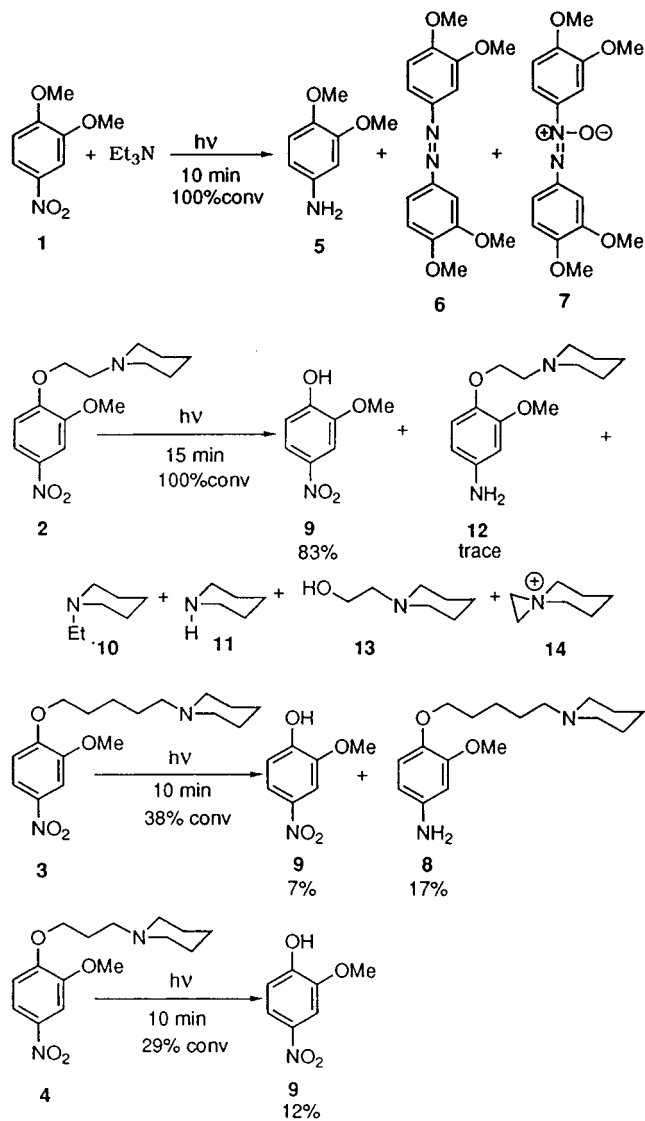
radical anions will only take place without problem if the spin density remains on the departing radical.

Radical anions of alkyl nitrophenyl ethers are stable toward fragmentation of the C–O bonds (Scheme 1A), and they generally follow alternative reaction pathways such as nitro group reduction¹⁸ or alkoxy group substitution via collapse of the radical ions.¹⁹ This observation has been rationalized considering the effect of the NO₂ group on the energy of the π^* state and on the spin density distribution in the radical anion (predictably concentrated in the NO₂ group).²⁰

We have recently shown that by altering (through Coulombic interactions) the electron density distribution of the intermediate nitroaryl ether radical anions, the intramolecular $\pi^*-\sigma^*$ electron transfer becomes easier due to the stabilization of the σ^* state. Then, the previously unknown reductive fragmentation of nitroaryl ethers can occur in aqueous solution.⁴ The model used avoids the use of metal cations and the “electrophilic catalysis” associated with them and consists of a 4-nitrophenoxy group linked through a short methylene chain to a tertiary amine (Scheme 1B). On the basis of theoretical calculations and few qualitative mechanistic experiments, we have proposed that a topologically controlled Coulombic interaction (TCCI) is created after a photoinduced intramolecular electron transfer process and that this interaction is responsible for the observed photocleavage.

Time-resolved electronic absorption spectroscopy has been used successfully to unravel the mechanisms of the photoreactions of nitrophenyl ethers in the presence of nucleophiles, mainly in aqueous solution.^{19b,21} The aim of the present paper is to clarify the mechanism of the “abnormal” photoinduced cleavage of 4-nitrophenyl piperidinoalkyl ethers (Scheme 1) by means of time-resolved transient absorption spectroscopy and, thereby, to gather support for the TCCI hypothesis advanced in our previous work.⁴

Scheme 2



Preparative Results

The substrates selected were 4-nitroveratrole (**1**), 1-piperidino-2-(2-methoxy-4-nitrophenoxy)ethane (**2**), 1-piperidino-5-(2-methoxy-4-nitrophenoxy)pentane (**3**), and 1-piperidino-3-(2-methoxy-4-nitrophenoxy)propane (**4**). In Scheme 2, the photolysis of substrates **2–4** in N₂ atmosphere and in acetonitrile as a solvent, as well as the corresponding photoreaction of 4-nitroveratrole in the presence of triethylamine, is described. These photoreactions have been previously described in aqueous solutions,^{4b} but the reaction intermediates were too short lived to be studied by time-resolved spectroscopy with our equipment (nanosecond laser flash photolysis). Therefore we tested other solvents where the TCCI could still be operative, but the different steps involved would be somewhat slower. Acetonitrile proved to be a good choice.

The photoreaction of 4-nitroveratrole (**1**) in the presence of triethylamine in acetonitrile (125 W medium-pressure Hg lamp, 10 min of irradiation, Pyrex filter, N₂ atmosphere) leads to complete consumption of the starting material and to a very complex reaction mixture where 3,4-dimethoxyaniline (**5**) could be identified as a major product, and 3,3',4,4'-tetramethoxyazobenzene (**6**) and 3,3',4,4'-tetramethoxyazoxybenzene (**7**) as two of the minor ones. Neither photosubstitution products nor 2-methoxy-4-nitrophenol could be detected in the reaction mixture.

(18) (a) Petersen, W. C.; Letsinger, R. L. *Tetrahedron Lett.* **1970**, 3509. (b) Dopp, D. *Topics Curr. Chem.* **1975**, 55, 49. (c) Marquet, J.; Moreno-Mañas, M.; Vallribera, A.; Virgili, A.; Bertrán, J.; Gonzalez-Lafont, A.; Lluch, J. M. *Tetrahedron*, **1987**, 43, 351. (d) Mir, M.; Marquet, J.; Cayón, E. *Tetrahedron Lett.* **1992**, 33, 7053.

(19) (a) Cantos, A.; Marquet, J.; Moreno-Mañas, M.; Castelló, A. *Tetrahedron* **1988**, 44, 2607. (b) van Eijk, A. M. J.; Huizer, A. H.; Varma, C. A. G. O.; Marquet, J. *J. Am. Chem. Soc.* **1989**, 111, 88. (c) Cantos, A.; Marquet, J.; Moreno-Mañas, M.; González-Lafont, A.; Lluch, J. M.; Bertrán, J. *J. Org. Chem.* **1990**, 55, 3303. (d) van Eijk, A. M. J.; Huizer, A. H.; Varma, C. A. G. O. *J. Photochem Photobiol. A: Chem.* **1991**, 56, 183.

(20) Martin, X.; Marquet, J.; Lluch, J. M. *J. Chem. Soc., Perkin Trans. 2* **1993**, 87.

(21) van Zeijl, P. H. M.; van Eijk, A. M. J.; Varma, C. A. G. O. *J. Photochem.* **1985**, 29, 415.

Substrate **3** (five methylene units linker) gave rise to 62% recovery of the starting material and 17% of the aniline **8** under similar conditions. Interestingly enough, a small amount (7% isolated yield) of 2-methoxy-4-nitrophenol (**9**) was produced.

2-Methoxy-4-nitrophenol (**9**) was the major product (83% isolated yield) when substrate **2** (two methylene units linker) was irradiated under the same conditions for 15 min. Qualitative analysis of the crude reaction by GC allowed the identification of *N*-ethylpiperidine (**10**), piperidine (**11**), and traces of both 1-piperidino-2-(4-amino-2-methoxyphenoxy)ethane (**12**), and 2-piperidinoethanol (**13**). One of the reviewers advanced the possibility that the 3-azoniaspiro[2.5]octane [$C_8H_{10}N^+C_2H_4$ (**14**)] ammonium cation was a primary product in this photoreaction and a precursor of 2-piperidinoethanol (**13**). We tested this hypothesis by carrying out the photoreaction in deuterated acetonitrile, monitoring directly its evolution by 1H NMR spectroscopy. The resulting spectrum was rather complex with some broad bands that suggested the presence of free radicals in low concentration, but certainly the cation **14** appeared to be one of the primary formed products derived from the alkylpiperidino chain (singlet at δ 2.9 for four protons, triplet at δ 3.2 for four protons, and multiplet centered at δ 1.7 for six protons) as established by the rather good coincidence of these values with the 1H NMR spectrum of an authentic sample (perchlorate as a counterion, δ 3.0, 3.3, and 1.8, respectively) prepared by an independent synthetic pathway (see Experimental Section). Direct analysis of the crude mixture by MS supported this conclusion since a distinct peak at m/e 112 [molecular peak for the 3-azoniaspiro[2.5]octane ammonium cation (**14**)] could be observed.

Substrate **4** showed a behavior intermediate between that of substrates **2** and **3**. Thus, a 12% yield of 2-methoxy-4-nitrophenol (**9**) was obtained after 10 min of irradiation under the same conditions. No reduction products were detected and 71% of the starting material (**4**) was recovered.

These results confirm that the TCCI hypothesis is also operating in acetonitrile as a solvent and under inert atmosphere, and that these conditions might be much more appropriate than aqueous solutions for our laser flash photolysis studies.

Laser Flash Photolysis Studies

In the discussion of the transient behavior of the photoexcited solution the following notation will be used. A particular set consisting of several types of molecular species A_i will be denoted by $\{A\}$. A particular compound B in its electronic state, labeled J, will be referred to as B(J). The electronic ground state, the n th excited singlet state, and the lowest triplet state will be referred to by $J = S_0$, $J = S_n$, and $J = T_1$ respectively. The contribution to the transient change in optical density (at wavelength λ when a single wavelength is monitored) induced by laser excitation of species B and arising from transient species $\{A\}$ at time t will be denoted by $\Delta OD(B, A, \lambda, t)$. The sum of all these contributions will be denoted by $\Delta OD(B, \lambda, t)$. A reference electronic absorption spectrum, e.g., of stable species of type R will be denoted by $OD(R, \lambda)$.

The transient absorption spectroscopy study has been carried out on the photoreactions of substrates **2** (C–O photocleavage) and **3** (NO_2 group photoreduction), and for the sake of comparison, on the photoreaction of NVT (**1**) with triethylamine.

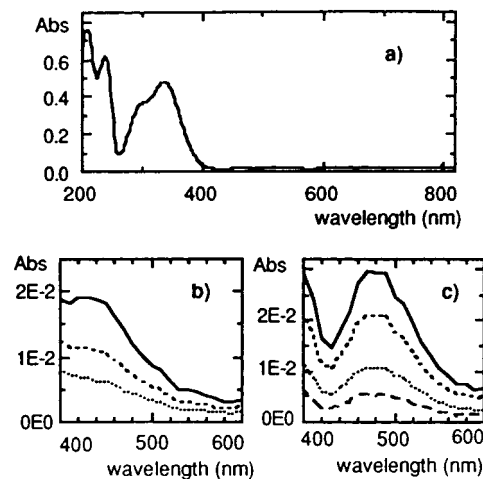


Figure 1. Electronic absorption spectra of a solution of 4-nitroveratrole (NVT, **1**) before and after laser excitation. (a) $OD(NVT, S_0, \lambda)$ in acetonitrile. (b) $\Delta OD(NVT, \lambda, t)$ in H_2O/CH_3CN (70:30 v/v) at different t after the laser pulse ($- t = 2.0 \times 10^{-7}$ s; $- - - t = 6.0 \times 10^{-7}$ s; $\cdots t = 1.0 \times 10^{-6}$ s). (c) $\Delta OD(NVT, \lambda, t)$ in CH_3CN at different t after the laser pulse ($- t = 8.0 \times 10^{-8}$ s; $- - - t = 2.0 \times 10^{-7}$ s; $\cdots t = 4.4 \times 10^{-7}$ s; $- - t = 6.8 \times 10^{-7}$ s).

1. The Triplet State of 4-Nitroveratrole [NVT (**1**)] in Acetonitrile.

The triplet state of NVT (**1**) in aqueous solution, without taking any precaution about the presence of oxygen, has been previously described by one of us.^{19b} However, preliminary work in acetonitrile under nitrogen showed an electronic absorption spectrum for the transient after the laser pulse, significantly different from that observed in aqueous solutions (Figure 1). Therefore, we decided to investigate the nature of this transient in acetonitrile and in N_2 atmosphere. The electronic absorption spectra $OD(NVT, S_0, \lambda)$ of NVT(S_0) is described in Figure 1a. The transient electronic spectra $\Delta OD(NVT, \lambda, t)$ of a solution of NVT in H_2O/CH_3CN (70:30 v/v) and pure CH_3CN at different t (time after the laser pulse) are depicted in Figure 1b and 1c, respectively (the wavelength region is limited to $\lambda > 400$ nm due to the large absorption of NVT(S_0) at shorter wavelengths that complicates the spectral analysis). In principle, the transient absorption in acetonitrile (Figure 1c) may contain contributions from several yet unidentified species X_1 . The point of time just after termination of the laser pulse will be denoted by t_L , and the point at which the transient absorption $\Delta OD(NVT, X_1, t)$ has vanished almost completely (i.e., $\Delta OD(NVT, X_1, t) < 0.001$) will be denoted by t_X . The decay of $\Delta OD(NVT, X_1, t)$ in period $t_L < t < t_X$ in acetonitrile and inert atmosphere is described by a single exponential function $\Delta OD(NVT, X, t) = \Delta OD(NVT, X, t_L) \exp\{-k_D(t - t_L)\}$.

Since $\Delta OD(NVT, X_1, t)$ vanishes completely after a single exponential decay, $\{X_1\}$ is taken to contain a single species X_1 . The value of k_D in acetonitrile and inert atmosphere is $4.59 \times 10^5 s^{-1}$ ($2.84 \times 10^6 s^{-1}$ under air atmosphere).

The transient absorption spectrum $\Delta OD(NVT, X_1, t)$ (Figure 1c) cannot be attributed to an intermediate in a photochemical reaction, because acetonitrile solutions of NVT do not change noticeably by steady state UV irradiation. The transient absorption is quenched by oxygen and piperylene. This is illustrated by the Stern–Volmer plot, shown in Figure 2a, for the quenching by piperylene. The rate constant k_q (piperylene) for quenching equals $1.57 \times 10^8 s^{-1}$.²²

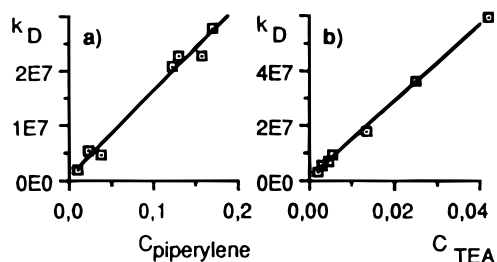


Figure 2. (a) Variation of the rate constant k_D for the decay of $\text{NVT}(T_1)$ as a function of $C_{\text{piperylene}}$. (b) Variation of the rate constant k_D for the decay of $\text{NVT}(T_1)$ as a function of C_{TEA} .

The decay constant k_D is not affected by variation of the laser energy (I_L) between 15 and 1.5 mJ. Therefore, bimolecular reactions between two transient species as well as between transient species and $\text{NVT}(S_0)$ are excluded. The decay constant k_D does not change when the concentration of NVT is varied. This means that excited states of multimers are not involved in the transient absorption.

The observed behavior of the decay constant of the transient absorption of NVT in acetonitrile indicates that the transient absorption $\Delta\text{OD}(\text{NVT}, X_1, t)$ is due to the population of $\text{NVT}(T_1)$. However, the composition of the solvent has a strong influence on k_D^{19b} and on the shape of the electronic spectrum of $\text{NVT}(T_1)$ (Figure 1). According to the literature,²³ we have attributed this behavior to hydrogen bonding to the NO_2 group of the triplet state molecule in aqueous solutions.

2. The Reaction of Triethylamine (TEA) with Photoexcited 4-Nitroveratrole [NVT (1)], in Acetonitrile. Preparative experiments indicate that neither photofragmentation nor stable photosubstitution products are formed when solutions of NVT and triethylamine (TEA) are irradiated with UV light at wavelengths longer than 290 nm. Only photoreduction products are observed in acetonitrile (Scheme 2). In agreement with these observations, the value of the triplet decay constant increases with increasing concentration of TEA in the acetonitrile solution. The rate constant $k_i(\text{TEA})$ for the bimolecular quenching of $\text{NVT}(T_1)$ by TEA in acetonitrile is found, from a Stern–Volmer plot (Figure 2b) of k_D versus C_{TEA} , to be $1.40 \times 10^9 \text{ M}^{-1} \text{ s}^{-1}$ (slightly higher than the value previously reported,^{18b} $0.46 \times 10^9 \text{ M}^{-1} \text{ s}^{-1}$ in $\text{H}_2\text{O}/\text{CH}_3\text{CN}$ (80:20 vv)).

In Figure 3a, the evolution of the transient spectrum $\Delta\text{OD}(\text{NVT}, X_1, \lambda, t)$ with time for a short period of time ($7 \times 10^{-7} \text{ s}$) after the laser pulse is shown. Global analysis of the complete kinetic data set (period of time $\approx 10^{-7} \text{ s}$ after the laser pulse) using GLint²⁴ only fits well to a mechanistic scheme of the $A \rightarrow B \rightarrow C$ type. This kinetic scheme is in agreement with the double exponential behavior followed by the decay of the transient spectrum at 470 nm in the same period of time

$$\Delta\text{OD}(\text{NVT}, \lambda, t) = \Delta\text{OD}(\text{NVT}, X, \lambda, t_L) \exp\{-k_{X_1}(t - t_L)\} + \Delta\text{OD}(\text{NVT}, Y, \lambda, t_X) \exp\{-k_{Y_1}(t - t_X)\}$$

(22) The triplet energy of 4-nitroveratrole (NVT) has not been measured. However, the corresponding value for 4-nitroanisole at 77 K in hydrocarbon solvents is $E_T = 60 \text{ kcal/mol}$ (Brinen, J. S.; Singh, B. *J. Am. Chem. Soc.* **1971**, *93*, 6623). A similar value for NVT would justify the relatively small k_q by piperylene ($E_T = 59 \text{ kcal/mol}$, Murov, S. L. *Handbook of Photochemistry*; Dekker: New York, 1973).

(23) Varma, C. A. G. O.; Plantenga, F. L.; Huizer, A. H.; Zwart, J. P.; Bergwerf, Ph.; van der Ploeg, J. P. M. *J. Photochem.* **1984**, *24*, 133.

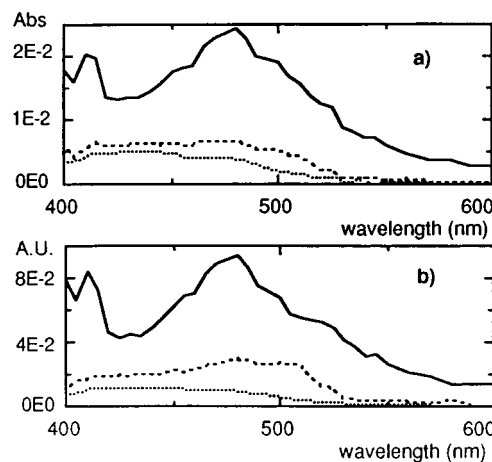
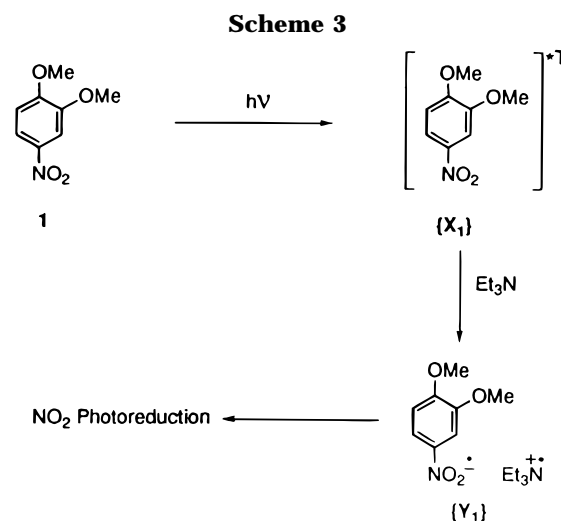


Figure 3. (a) Transient absorption spectrum $\Delta\text{OD}(\text{NVT}, \lambda, t)$ of the laser-excited solution of NVT in acetonitrile containing TEA ($-t = 3.0 \times 10^{-8} \text{ s}$; $--- t = 1.0 \times 10^{-7} \text{ s}$; $\cdots t = 7.0 \times 10^{-7} \text{ s}$). (b) Absorption spectrum of the transient species $\{X_1\}$ $—$, $\{Y_1\}$ $---$, and $\{Z_1\}$ \cdots , after GLint²⁴ analysis of the complete experimental data set according to the kinetic model $A \rightarrow B \rightarrow C$.



The first species in the kinetic scheme, $\{X_1\}$ ($\lambda_{\text{max}} \approx 475\text{--}495 \text{ nm}$) can be assigned to the $\text{NVT}(T_1)$ on the basis of its absorption spectrum (compare the solid line in Figure 3b with Figure 1c). $\text{NVT}(T_1)$ evolves into a second transient, $\{Y_1\}$ (dashed line in Figure 3b), the absorption spectrum of which resembles the spectrum of the radical anion²⁵ of NVT with respect to both the maximum of the band at 490 nm and the tail of the UV band. Therefore, we identify $\{Y_1\}$ with the NVT radical anion. Strong support for this assignment came from the observed quenching of $\{Y_1\}$ by *m*-dinitrobenzene (*m*-DNB) (good redox trap that does not interact with $\text{NVT}(T_1)$ ^{19b} and that does not absorb significantly at 355 nm). This quenching was accompanied by the appearance of a new absorption ($\lambda_{\text{max}} \approx 500 \text{ nm}$) attributed to the *m*-DNB radical anion.²⁶ Within a few nanoseconds after time t_X ,

(24) GLint is a form of global analysis developed by Applied Photophysics Ltd. that allows a complete data set, comprising kinetic records obtained over a range of wavelengths, to be analyzed according to whatever reaction scheme is thought to be appropriate. GLint uses the Marquardt–Levenberg algorithm and 4th order Runger–Kutta numerical integration. Carey, M. *EPA Newslett.* **1994**, *52*, 21.

(25) Mutai, K.; Yokoyama, K.; Kanno, S.; Kobayashi, K. *Bull. Chem. Soc. Jpn.* **1982**, *55*, 1112.

(26) (a) Bellobono, I. R.; Gamba, A.; Sala, G.; Tampieri, M. *J. Am. Chem. Soc.* **1972**, *94*, 5781. (b) Mohammad, M. *J. Chem. Soc., Perkin Trans. 2* **1975**, 526.

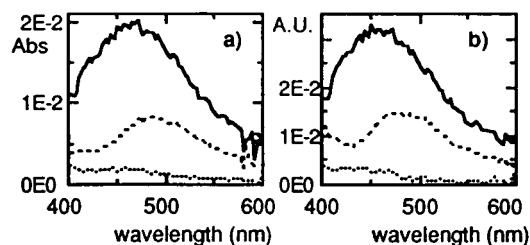


Figure 4. (a) Transient absorption spectrum $\Delta OD(2, \lambda, t)$ of the laser-excited solution of product **2** in acetonitrile ($-t = 4.0 \times 10^{-8}$ s; $--- t = 2.0 \times 10^{-7}$ s; $\cdots t = 2.4 \times 10^{-7}$ s). (b) Absorption spectrum of the transient species $\{X_2\}$ —, $\{Y_2\}$ ---, and $\{Z_2\}$ \cdots , after GLint²⁴ analysis of the complete experimental data set according to the kinetic model $A \rightarrow B \rightarrow C$.

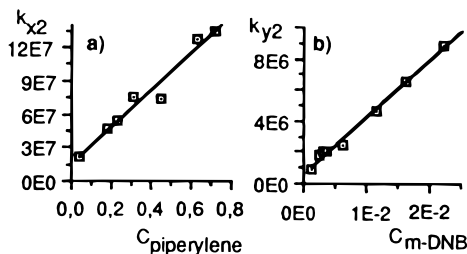
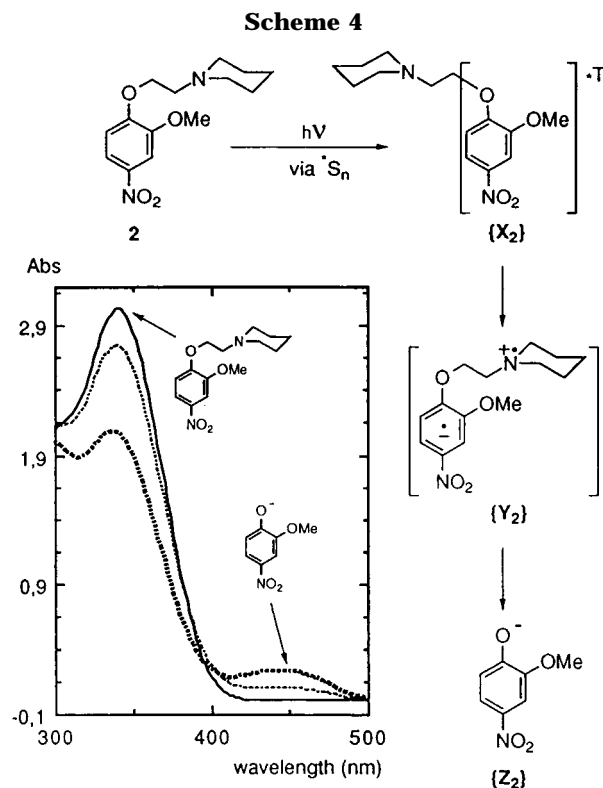


Figure 5. (a) Variation of the rate constant k_{X_2} for the decay of **2**(T₁) as a function of $C_{\text{piperylene}}$. (b) Variation of the rate constant k_{Y_2} for the decay of $\{Y_2\}$ as a function of $C_{m\text{-DNB}}$.

species $\{Y_1\}$ is converted into new species $\{Z_1\}$ (dotted line in Figure 3b). Species $\{Y_1\}$ (NVT radical anion) decays to $\{Z_1\}$ in a monoexponential manner with a decay rate constant $k_{Y_1} = 1.1 \times 10^7 \text{ s}^{-1}$. When a longer period of time is monitored ($\approx 10^{-4}$ after the laser pulse) the decay of species $\{Z_1\}$ can be observed ($k_{Z_1} = 4.53 \times 10^5 \text{ s}^{-1}$). Since species $\{Z_1\}$ are nonpersistent, we assume they are intermediates in the photoreduction reaction (Scheme 3).

3. The Photolysis of 1-Piperidino-2-(2-methoxy-4-nitrophenoxy)ethane (2) in Acetonitrile. The preparative photolysis of 1-piperidino-2-(2-methoxy-4-nitrophenoxy)ethane (**2**) in acetonitrile and inert atmosphere leads to formation of the 2-methoxy-4-nitrophenolate anion (Scheme 2). The evolution of the transient spectrum with time after the laser pulse is shown in Figure 4a. Global analysis of the complete kinetic data set using GLint²⁴ fits well only with a mechanistic scheme of the $A \rightarrow B \rightarrow C$ type. In contrast with the previously described photoreaction of **1**, in this case the last transient is totally persistent over the whole period of time monitored ($\approx 10^{-4}$ s after the laser pulse). This kinetic scheme is in accordance with the double exponential behavior observed for the decay of the transient spectrum at 469 nm. The first transient, X_2 , with absorption spectrum $\Delta OD(2, X_2, t_i)$, was assigned to **2**(T₁) on the basis of its lifetime ($k_{X_2} = 1.30 \times 10^7 \text{ s}^{-1}$) and its quenching by piperylene. The Stern–Volmer plot for the quenching of the transient absorption $\Delta OD(2, X_2, t_i)$ by piperylene is shown in Figure 5a. The rate constant k_q (piperylene) for quenching is $1.67 \times 10^8 \text{ s}^{-1}$.²² Interestingly enough, **2**(T₁) shows $\lambda_{\text{max}} \approx 450\text{--}470$ nm, significantly lower than the corresponding value for NVT(T₁) (λ_{max} around 490 nm, Figure 1).

After the disappearance of **2**(T₁), the spectrum represented by the dashed line in Figure 4b and denoted by $\Delta OD(2, Y_2, t_x)$ is observed. The species that give rise to this spectrum will be denoted by $\{Y_2\}$. We assigned



species $\{Y_2\}$ to a zwitterionic radical anion/radical cation intramolecular pair (Scheme 4). Within a few microseconds after time t_x species $\{Y_2\}$ are converted into new species $\{Z_2\}$. Species $\{Y_2\}$ decays to $\{Z_2\}$ in a monoexponential manner with a decay rate constant k_{Y_2} equal to $4.48 \times 10^5 \text{ s}^{-1}$. Assignment of species $\{Y_2\}$ to the intramolecular radical ion pair was supported by the good correlation (Figure 5b) observed in a Stern–Volmer plot of k_{Y_2} versus $C_{m\text{-DNB}}$ [*m*-dinitrobenzene (*m*-DNB)]. The rate constant k_q (*m*-DNB) for quenching is $3.65 \times 10^8 \text{ s}^{-1}$. Species $\{Z_2\}$ are totally persistent. This fact, together with the features of the observed absorption spectrum ($\lambda_{\text{max}} \approx 430\text{--}450$ nm, Figure 4b), led us to propose the structure of 2-methoxy-4-nitrophenolate anion, the final product in the preparative photolysis (Scheme 4), for species $\{Z_2\}$.

The photolysis of **2** in an air-saturated solution was also investigated. In this case no species $\{Z_2\}$ are observed. We postulate that the intramolecular radical ion pair is quenched by the presence of oxygen, thus precluding the production of the 2-methoxy-4-nitrophenolate. In Scheme 5, a mechanistic pathway is proposed, and the corresponding rate constants are described. This result is further support for the assignment of species $\{Y_2\}$ to the structure of the intramolecular radical ionic pair.

4. The Photolysis of 1-Piperidino-5-(2-methoxy-4-nitrophenoxy)pentane (3) in Acetonitrile. The preparative photolysis of 1-piperidino-5-(2-methoxy-4-nitrophenoxy)pentane (**3**) in acetonitrile and inert atmo-

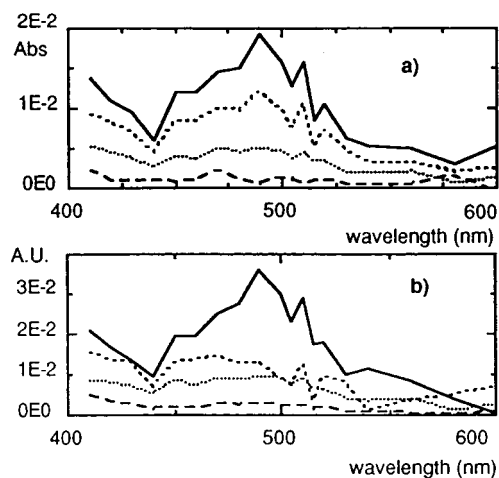


Figure 6. (a) Transient absorption spectrum $\Delta OD(3, \lambda, t)$ of the laser-excited solution of product **3** in acetonitrile ($-t = 3.0 \times 10^{-8}$ s; $--- t = 6.0 \times 10^{-8}$ s; $\cdots t = 3.0 \times 10^{-7}$ s; $- \cdot - t = 6.0 \times 10^{-6}$ s). (b) Absorption spectrum of the transient species $\{X_3\}$ —, $\{Y_3\}$ ---, $\{Z_3\}$ \cdots , and $\{W_3\}$ — \cdot — after GLint²⁴ analysis of the complete experimental data set according to the kinetic model $A \rightarrow B \rightarrow C \rightarrow D$.

sphere leads mainly to photoreduction of the nitro group and to a small amount of 4-nitrophenolate anion (Scheme 2). In Figure 6a, the evolution of the transient spectrum with time after the laser pulse is described. In this case, to get a good fit in the global analysis of the complete kinetic data set (time period $\approx 10^{-6}$ s after the laser pulse) using GLint,²⁴ a kinetic scheme of the $A \rightarrow B \rightarrow C \rightarrow D$ type had to be postulated (this was the simplest scheme that gave a fit good enough). This kinetic scheme is in agreement with the triple exponential behavior followed by the decay of the transient spectrum at 470 nm in the same period of time

$$\Delta OD(3, X, \lambda, t_L) \exp\{-k_{X_3}(t - t_L)\} + \Delta OD(3, Y, \lambda, t_X) \exp\{-k_{Y_3}(t - t_X)\} + \Delta OD(3, Z, \lambda, t_Y) \exp\{-k_{Z_3}(t - t_Y)\}$$

In contrast with the previously described photoreaction of **2**, the last transient was not persistent when it was monitored for a longer period of time ($\approx 10^{-4}$ s after the laser pulse). The first transient, X_3 , with absorption spectrum $\Delta OD(3, X_3, t_L)$, was assigned to **3**(T₁) on the basis of its absorption spectrum ($\lambda_{\max} \approx 490$ nm, very similar to NVT(T₁)), lifetime ($k_{X_3} = 2.75 \times 10^7$ s⁻¹) and its quenching by piperylene.

After the disappearance of **3**(T₁), the spectrum represented by the dashed line in Figure 6b and denoted by $\Delta OD(3, Y_3, t_X)$ is observed. The species that gives rise to this spectrum will be denoted by $\{Y_3\}$. Species $\{Y_3\}$ decays rapidly to $\{Z_3\}$ in a monoexponential manner with a decay rate constant $k_{Y_3} = 1.45 \times 10^7$ s⁻¹. Within a few microseconds after time t_X , species $\{Z_3\}$ is converted into new species $\{W_3\}$ (monoexponential decay, $k_{Z_3} = 2.8 \times 10^6$ s⁻¹). The nature of species $\{Y_3\}$ and $\{Z_3\}$ was investigated using methylviologen (MV²⁺) as a redox trap (MV²⁺ does not significantly interact with the excited triplet state of nitrophenyl ethers and does not absorb at 355 nm).^{19b} In the presence of MV²⁺ ($C_{MV} = 1.22 \times 10^{-4}$ M) the decay of the transient spectrum at 470 nm follows a double exponential function in the time period of 10^{-6} s after the laser pulse. Species $\{Y_3\}$ is now not observed, suggesting that it is effectively quenched by MV²⁺, its decay being indistinguishable from the decay

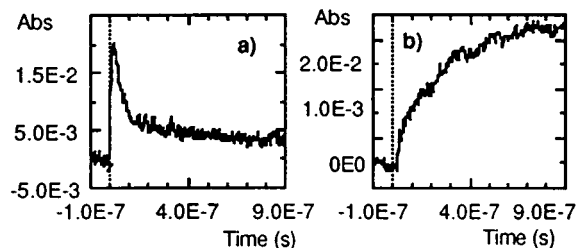


Figure 7. Decay (a) of the transient spectrum $\Delta OD(3, \lambda, t)$ in the presence of MV²⁺, monitored at $\lambda = 470$ nm and compared (b) with the rate of formation of MV⁺ monitored at 602 nm.

of $\{X_3\}$. Therefore, the observed rate constant $k_{q(Y_3)}[MV^{2+}] \geq 2.7 \times 10^7$ s⁻¹ under these conditions. The second transient has been assigned to $\{Z_3\}$. The decay of species $\{Z_3\}$ is also accelerated in the presence of MV²⁺. Thus, species $\{Z_3\}$ decays to $\{W_3\}$ in a monoexponential manner with an observed rate constant $k_{q(Z_3)}[MV^{2+}] = 6.0 \times 10^6$ s⁻¹. These results suggest that both transient species $\{Y_3\}$ and $\{Z_3\}$ are probably intramolecular radical-ion pairs but of different structure. In the case of $\{Z_3\}$ this conclusion is supported by the good correlation observed in a Stern–Volmer plot of k_{Z_3} versus C_{MV} .

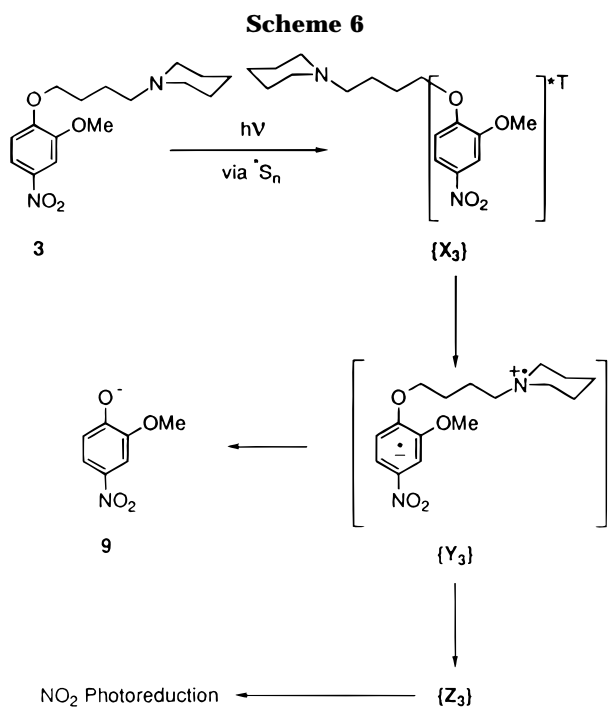
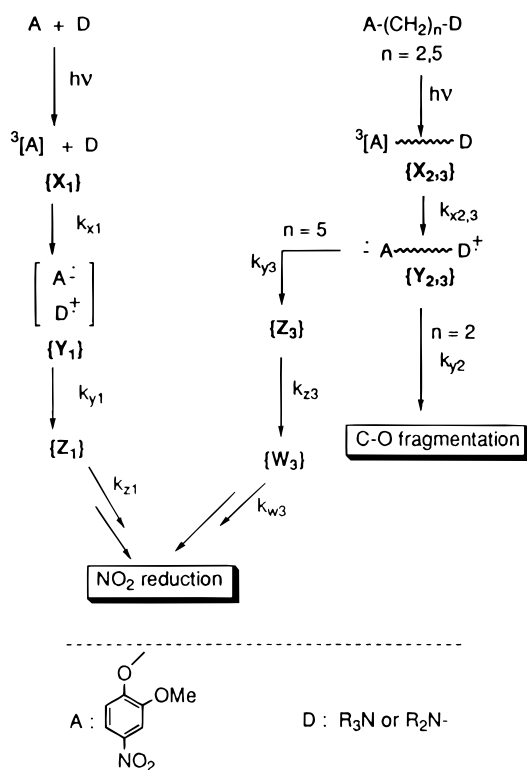
In Figure 7 we show that the decay of the transient spectrum at 470 nm in the presence of MV²⁺ nicely correlates with the formation of MV⁺ (appearance of the band at $\lambda_{\max} = 602$ nm corresponding to the MV⁺).²⁷ Thus, the transient absorption band $\Delta OD(MV^+, \lambda, t)$ due to MV⁺ grows from zero to its maximum intensity within a period of time after the laser pulse ($\approx 6 \times 10^{-7}$ s) coinciding with the decay period of $\{Z_3\}$ in the same conditions ($\approx 5 \times 10^{-7}$ s). In addition, the growth of $\Delta OD(MV^+, \lambda, t)$ can be described by a double exponential function

$$\Delta OD(MV^+, \lambda, t) = \Delta OD(MV^+, \lambda, t_Y) \{1 - \exp[-k_{MV}(t - t_Y)]\} + \Delta OD(MV^+, \lambda, t_Z) \{1 - \exp[-k'_{MV}(t - t_Z)]\}$$

The rise time of MV⁺, $k_{MV} = 1.18 \times 10^7$ s⁻¹ and $k'_{MV} = 3.69 \times 10^6$ s⁻¹ at the particular value for the concentration C_{MV} of MV²⁺ used, almost perfectly matches the expected values $k_{q(Y_3)}[MV^{2+}] - k_{Y_3} = 1.25 \times 10^7$ s⁻¹ and $k_{q(Z_3)}[MV^{2+}] - k_{Z_3} = 4.19 \times 10^6$ s⁻¹, considering species $\{Y_3\}$ and $\{Z_3\}$ as the exclusive responsible for the MV⁺ formation.

The spectrum $\Delta OD(3, Y_3, t_X)$ ($\lambda_{\max} \approx 450$ – 470 nm) is quite similar to $\Delta OD(2, Y_2, t_X)$ observed in the photolysis of compound **2**, whereas the spectrum $\Delta OD(3, Z_3, t_Y)$ ($\lambda_{\max} \approx 480$ – 500 nm) is more similar to $\Delta OD(NVT, Y_1, \lambda, t_X)$ observed in the photoreaction of NVT (**1**) with triethylamine. Considering these facts, it seems that $\{Y_3\}$ corresponds to an intramolecular radical-ion pair with similar properties to the species $\{Y_2\}$ observed in the photolysis of substrate **2**, and susceptible to C–O bond cleavage. The cleavage process is in this case (probably due to the conformational freedom of substrate **3**) in competition with the fast evolution to species $\{Z_3\}$ (intermediate also with good reducing properties), perhaps another radical-ion pair with different geometry probably belonging to the pathway leading to photoreduction products (Scheme 6). It should be remembered that photoreduction is the main observed reaction in the preparative experiments with this substrate.

(27) Duonghong, D.; Borgarello, E.; Graetzel, M. *J. Am. Chem. Soc.* **1981**, *103*, 4685.

**Scheme 7**

group reduction products by proton transfer²⁸ in the radical ion pair ($k_{Y1} = 1.1 \times 10^7 \text{ s}^{-1}$), a probable structure will correspond to an ion-radical pair with the aminium moiety near the NVT nitro group. On the other hand, substrate **2** leads to C–O bond photocleavage in a relatively slow process ($k_{Y2} = 4.5 \times 10^5 \text{ s}^{-1}$) through intermediate species {Y₂} that also shows radical-ion pair (intramolecular in this case) behavior. However, its absorption spectrum ($\lambda_{\text{max}} = 460\text{--}480 \text{ nm}$), its reactivity (C–O bond breaking), and the fact that now the motion of the aminium moiety in the radical-ion pair is limited by the short length of the linker leads to the conclusion that species {Y₂} have different geometry than species {Y₁} observed in the photoreaction of NVT (**1**) with TEA. The aminium radical cation moiety in {Y₂} is remote from the nitro group. Confirmation of these conclusions comes from the results of the photolysis of substrate **3**. This product has a long spacer (five methylene units) and, therefore, there are no serious restrictions for the radical-ion pair to adopt the geometry with the aminium moiety close to the nitro group. Accordingly, nitro group photoreduction is the main observed process in this case, but a small, although significant, yield of the product from C–O bond cleavage can be observed in the preparative photolysis. The laser flash photolysis studies indicate the presence of two transient species {Y₃} and {Z₃} with good reducing properties in a period of time $\approx 10^{-7} \text{ s}$ after the laser pulse. The first one {Y₃} decays rapidly ($k_{Y3} = 1.45 \times 10^7 \text{ s}^{-1}$) to the second one {Z₃}, and its redox properties and absorption spectrum ($\lambda_{\text{max}} = 460\text{--}470 \text{ nm}$) suggest an intramolecular radical-ion pair structure with geometry similar to {Y₂}, with the aminium moiety away from the nitro group. This transient species {Y₃} seems to be responsible for the minor proportion of C–O bond cleavage observed in the preparative photolysis of substrate **3**. The second one {Z₃} has a decay rate constant ($k_{Z3} = 2.8 \times 10^6 \text{ s}^{-1}$) and a different absorption spectrum ($\lambda_{\text{max}} = 480\text{--}500 \text{ nm}$), rather similar to {Y₁}. Therefore, it could be tentatively assigned to another intramolecular radical-ion pair with different geometry (i.e. the aminium moiety close to the nitro group) or to any of the intermediates with good reducing properties encountered in the reduction of a nitro group to an amine. This transient species {Z₃} would be responsible for the nitro group photoreduction observed as a major process in the preparative photoreaction. A general mechanistic scheme for the photoreactions studied is proposed in Scheme 7, and the measured rate constants involved in the different steps are collected in Table 1.

The preparative photoreaction of substrate **2** in acetonitrile has allowed us to detect and identify several products derived from the piperidinoalkyl moiety after fragmentation (Scheme 2). In Scheme 8, a rationale for the production of the different detected products from a common intermediate is shown. The simultaneous appearance of the cyclized cation **14** (path A, Scheme 8), piperidine (**11**) (elimination on **14** and hydrolysis of the resulting enamine), and 2-piperidinoethanol (**13**) (substitution on **14**) on one side, and the reduced product ethylpiperidine (**10**) (path B, Scheme 8) on the other side, strongly support the intermediacy of the ethylpiperidinium diradical cation as the primary product in the mesolytic fragmentation step of substrate **2**.

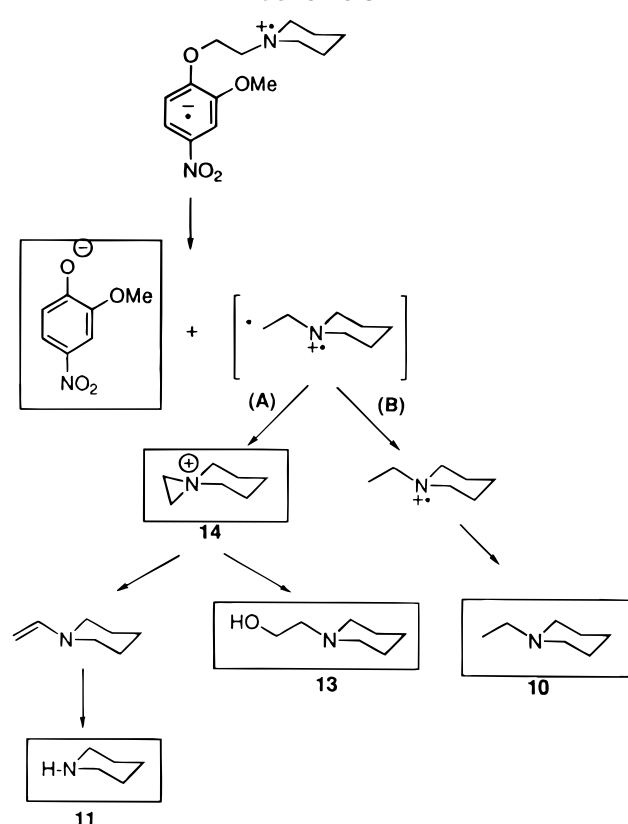
In conclusion, this work confirms earlier^{2,4} provisional interpretations on the importance of the TCCI effects in

(28) (a) Pacifici, G.; Irick, G.; Anderson, C. *J. Am. Chem. Soc.* **1970**, *91*, 213. (b) Döpp, D.; Müller, D.; Sailer, K.-H. *Tetrahedron Lett.* **1974**, 2137.

Table 1. Values of the k_D for the Decay of the Transient Species^a

photoreaction	$k_X \times 10^{-5} \text{ s}^{-1}$	$k_Y \times 10^{-5} \text{ s}^{-1}$	$k_Z \times 10^{-5} \text{ s}^{-1}$	$k_W \times 10^{-5} \text{ s}^{-1}$
1 + $h\nu$	4.59 ± 0.01	—	—	—
1 + TEA + $h\nu$	(14000 ± 231) ^b	110 ± 14	4.53 ± 0.09	—
2 + $h\nu$	158 ± 1	4.48 ± 0.02	^c	—
3 + $h\nu$	275 ± 22	145 ± 23	28 ± 4	3.3 ± 1.8

^a Rate constants defined by more than 450 data points (ref 24) and standard errors. ^b Bimolecular constant, $\text{M}^{-1} \text{ s}^{-1}$, from Figure 2. The standard error in the individual k_{obs} was less than 5% in all the cases. ^c Stable species.

Scheme 8

governing the reactivity of a charged intermediate. It also shows that in our substrates the TCCI induced C–O bond cleavage is a relatively slow process only observable if the aminium cation moiety has restricted freedom of motion.

Experimental Section

General Considerations. ¹H NMR were recorded at 250 or 400 MHz and the ¹³C NMR at 62.5 or 100 MHz. 4-Nitroveratrole was prepared by nitration of veratrole.²⁹ Potassium 2-methoxy-4-nitrophenoxide was prepared according to the method of Pollenoff and Robinson.³⁰ 1-Piperidino-2-(2-methoxy-4-nitrophenoxy)ethane, **2**, 1-piperidino-5-(2-methoxy-4-nitrophenoxy)pentane, **3**, and 1-piperidino-3-(2-methoxy-4-nitrophenoxy)propane, **4**, were prepared as previously described by some of us.⁵ All flash photolysis experiments and photochemical irradiations were carried out in nitrogen or argon saturated solutions. Laser flash photolysis experiments were performed using an LKS50 instrument from Applied Photophysics. A Q-switched Nd:YAG laser (Spectron Laser Systems, UK; pulse width ca. 9 ns) at 355 nm was used for laser flash excitation. Typically 5–15 mJ/pulse were used for sample excitation.

General Procedure for the Photochemical Reactions Described in Scheme 2. In a 300 mL photochemical reactor,

1 mmol of substrate dissolved in 300 mL of distilled acetonitrile was introduced. The solution was degassed by bubbling nitrogen or argon for 30–60 min and irradiated with a 125 W medium-pressure Hg lamp at room temperature for 10–15 min, following its evolution by GLC. The solvent was evaporated, the residue was dissolved in 50 mL of chloroform, and the organic solution was successively extracted with 1 M NaOH and with 1 M HCl. The aqueous basic layer was acidified, the aqueous acid one was basified, and then both layers were extracted with chloroform. All organic layers were dried, and the solvent was evaporated. Phenols were obtained directly from basic medium extractions. Anilines were obtained from acid medium extractions. All other reaction products were obtained from the residue of the initial extraction after column chromatography through silica gel (230–400 mesh) using mixtures of chloroform/ethyl acetate as eluent. In the different reactions described in Scheme 2 the following products were obtained with the yields given in the text: piperidine (**11**), *N*-ethylpiperidine (**10**), and 2-piperidinoethanol (**13**), identified by comparison with commercially available authentic samples; 3,4-dimethoxyaniline (**5**), 3,3',4,4'-tetramethoxyazobenzene (**6**), and 2-methoxy-4-nitrophenol (**9**), all of them previously described by us;⁵ 3-azoniaspiro[2.5]octane cation (**14**) identified by comparison with an authentic sample of 3-azoniaspiro[2.5]octane perchlorate³¹ synthesized following the procedure reported in the literature; 1-piperidino-5-(4-amino-2-methoxyphenoxy)pentane (**8**) was isolated by column chromatography and purified by distillation (175–200 °C oven temperature, 0.05 Torr): IR (KBr) 3300, 2934, 2856, 1620, 1512, 1455, 1276, 1260 cm^{-1} ; ¹H NMR (CDCl_3) δ 1.55 (m, 10H), 1.77 (m, 2H), 2.40 (m, 6H), 3.80 (s, 3H), 3.95 (t, $J = 6$ Hz, 2H), 6.17 (dd, $J = 3$ Hz, $J = 8$ Hz, 1H), 6.26 (d, $J = 3$ Hz, 1H), 6.75 (d, $J = 8$ Hz, 1H); ¹³C NMR (CDCl_3) δ 24.1, 24.3, 25.6, 26.4, 29.3, 54.5, 55.8, 59.3, 70.1, 100.9, 106.6, 115.9, 140.9, 141.4, 151.4; MS m/z (relative intensity) 292 (M^+ , 1), 154 (64), 110 (8), 98 (100); 1-piperidino-2-(4-amino-2-methoxyphenoxy)ethane, **12**, was isolated by column chromatography and purified by distillation (150–160 °C oven temperature, 0.05 Torr): IR (KBr) 3358, 2934, 1625, 1593, 1512, 1466, 1457, 1297 cm^{-1} ; ¹H NMR (CDCl_3) δ 1.55 (m, 6H), 2.50 (m, 4H), 2.75 (t, $J = 6$ Hz, 2H), 3.80 (s, 3H), 4.14 (t, $J = 6$ Hz, 2H), 6.17 (dd, $J = 3$ Hz, $J = 8$ Hz, 1H), 6.26 (d, $J = 3$ Hz, 1H), 6.75 (d, $J = 8$ Hz, 1H); ¹³C NMR (CDCl_3) δ 24.1, 25.7, 54.9, 55.7, 57.9, 67.9, 100.9, 106.6, 116.4, 141.3, 141.4, 150.7; MS m/z (relative intensity) 250 (M^+ , 2), 137 (3), 112 (74), 110 (10), 98 (100).

General Procedure for the Laser Flash Photolysis Experiments. A sample was prepared with an absorbance of about 0.5 at 355 nm, degassed by bubbling nitrogen for 30 min and analyzed with the previously described Laser Kinetic Spectrometer LKS 50. For the Stern–Volmer diagrams with piperylene as quencher, samples were degassed by six freeze-pump-thaw cycles for volatility reasons. Before and after degassing UV spectra were recorded in order to calculate the concentration of piperylene using its known ϵ value.

Acknowledgment. We thank Prof. M. Chanon for helpful discussions. Financial support from DGCYT (MEC of Spain) through project PB93-0895, and from “Generalitat de Catalunya” through the projects GRQ93-2070 and 1995SGR 00469 is gratefully acknowledged.

JO961821I

(29) Vermeulen, M. H. *Recl. Trav. Chim. Pays-Bas* **1906**, 25, 12.

(30) Pollenoff, F.; Robinson, R. *J. Chem. Soc.* **1918**, 113, 645.

(31) Leonard, N. J.; Paukstellis, J. V. *J. Org. Chem.* **1965**, 30, 821.